500451-1001 PATENT

IN THE UNITED STATES PATENT AND TRADEMARK OFFICE

6/w.m. 5/22/03

Inventors: Eric W. McFarland

Serial No.: 10/057,223

Filing Date: January 25, 2002

Group No.: 1753

Examiner: Alan D. Diamond

For: APPARATUS AND METHOD FOR PHOTOVOLTAIC ENERGY PRODUCTION BASED ON INTERNAL CHARGE EMISSION IN A SOLID-STATE HETEROSTRUCTURE

Box: RESPONSE
Assistant Commissioner for Patents
Washington, D.C. 20231

Sir:

RESPONSE

Responsive to the Office Action mailed May 14, 2003, in the above-captioned application, enclosed are the omitted references: "Clean Electricity from Photovoltaics" and "Physics of Semiconductor Devices, Second Edition". Each document includes the title page, the copyright page, and the relevant substantive pages comprising the document.

Respectfully submitted,

MICHAEL A. O'NEIL, P.C.

Michael A. O'Neil
Registration No. 23,007

Date: May 19th, 2003
5949 Sherry Lane, Suite 820
Dallas, Texas 75225
(214) 739-0088
(214) 739-8284 (Fax)

response re 500451-1001.wpd

Series on Photoconversion of Solar Energy — Vol. 1

CLEAN ELECTRICITY FROM PHOTOVOLTAICS

Editors

Mary D. Archer
Imperial College, UK

Robert Hill
University of Northumbria, UK

ICP

Imperial College Press

Published by

Imperial College Press
57 Shelton Street
Covent Garden
London WC2H 9HE

Distributed by

World Scientific Publishing Co. Pte. Ltd.
P O Box 128, Farrer Road, Singapore 912805
USA office: Suite 1B, 1060 Main Street, River Edge, NJ 07661
UK office: 57 Shelton Street, Covent Garden, London WC2H 9HE

British Library Cataloguing-in-Publication Data
A catalogue record for this book is available from the British Library.

Index prepared by Indexing Specialists, Hove, BN3 2DJ, UK

CLEAN ELECTRICITY FROM PHOTOVOLTAICS
Series on Photoconversion of Solar Energy — Vol. 1

ISBN 1-86094-161-3

Printed in Singapore.

with Ge, whereas alloying with C results in a higher band gap. These double or triple junctions extend the spectral sensitivity and, in addition, improve the stability of the cells as compared to the single-junction case.

Table 3.2 Prominent efficiencies obtained with monolithic multijunction cells

Cell structure	Efficiency	Reference
GaInP/GaAs,	30.3 (AM1.5)	Takamoto, 1997
GaInP/GaAs/Ge	25.7 (AM0)	Bertness, 1994
AlGaAs/GaAs	27.6 (AM1.5)	Chung, 1990
a–Si / a–SiGe / a–SiGe *	13 (AM1.5)	Yang, 1997
Micromorph **	12 (AM1.5)	Shah *et al.*, 1997

*= stabilised efficiency; ** = combination of an a–Si:H top cell and a small-grain polycrystalline Si bottom cell grown by very high-frequency glow discharge.

3.2.3 *Metal–semiconductor and metal–insulator–semiconductor junctions*

The two previous sections considered junctions between two semiconductors. In principle, a *metal–semiconductor junction* (Schottky diode) with rectifying properties would also be suitable for the construction of a solar cell. When the optical transparency of the thin metal layer is sufficient, the photons, penetrating into the semiconductor, generate electron–hole pairs, which are separated by the field in the depletion layer at the metal–semiconductor surface (see Fig. 3.4).

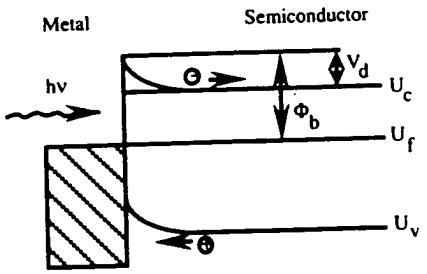

Figure 3.4 Band-gap diagram for a typical Schottky junction, realised on an *n*-type semiconductor. Under illumination, the holes are collected by the field in the depletion layer near the metal–semiconductor junction.

Although at first sight attractive from the point of view of ease of production, this approach suffers from limitations caused by the high dark currents flowing in such structures as compared to the heterojunction approach discussed above. These high dark currents are composed of majority carriers which flow by thermionic emission over the barrier ϕ_b (see Fig. 3.4) as given by

$$i_o = A^{**}T^2 \exp\left(\frac{-q\phi_b}{kT}\right)\left[\exp\left(\frac{qV}{kT}\right)-1\right] \tag{3.2}$$

where A^{**} is the Richardson constant and V is the forward bias over the metal–semiconductor junction. In addition, the barrier height is reduced by image effects that are a function of the doping level. Even when assuming 100% light transmission through the metal, the predicted efficiency of solar cells based on metal–semiconductor junctions will be below 10% (see *e.g.* Hovel, 1975). A relatively new approach to overcome this limitation consists in using the absorption in the thin metal layer to excite 'hot carriers' over the barrier. Schmidt (1994) predicted that this could enhance the efficiency by 10%, but no experimental confirmation of this approach has yet been reported. From the technological point of view, it is not straightforward to realise metal–semiconductor junctions with reproducible barrier heights, because these are strongly influenced by interfacial contamination and crystal orientation. However, the interpolation of an interfacial oxide between the metal and semiconductor can be used advantageously to increase the barrier height and thereby

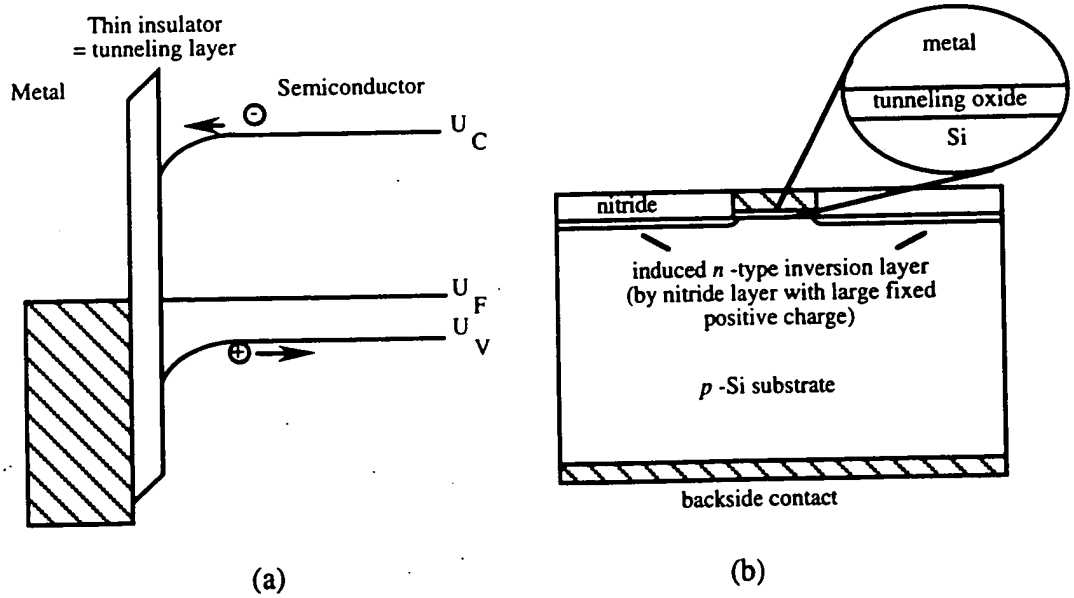

Figure 3.5 (a) Band-gap diagram for a cell with an MIS contact under equilibrium conditions; (b) Schematic cross-section of an MIS–IL Si cell.

decrease the dark current. When this approach is used, the thickness (2–4 nm) of the oxide is chosen so that the minority carriers can tunnel through the oxide (see the band-gap scheme of Fig. 3.5a). Such a device is called a *metal–insulator–semiconductor* (MIS) solar cell.

Much effort has gone into the development of Si MIS-technology. The most popular design is the MIS-inversion layer (IL) cell (see Fig. 3.5b). This cell configuration is realised by depositing a nitride layer, containing a large fixed positive charge, on a *p*-type Si-substrate. This induces an *n*-type inversion-type emitter, which is contacted through an MIS contact. An alternative is the MIS-contacted n^+-*p* Si solar cell. The ongoing research to optimise the latter MIS-approach has resulted in cell efficiencies above 20% (see Metz, 1997) and efficiencies as high as 23% are predicted (Kuhlmann, 1997) for a MIS-inversion layer cell.

3.3 Optical design of cells

This section on optical cell design is divided into two parts. Section 3.3.1 deals with the design of the front and back surfaces to ensure that the light is efficiently coupled into the cell body. Different light-trapping schemes and their practical implementation are reviewed. Section 3.3.2 deals with the properties of anti-reflective coatings.

The optical optimisation of cell surfaces divides into two questions: how can light be coupled efficiently into the cell and how can it be kept in the cell once it has entered the cell to ensure maximal absorptance? The first question basically addresses the reduction of the primary reflectance of the front surface whereas the second is related to the development of light-trapping schemes. The second item will be dealt with first because the light-trapping schemes discussed also affect the front-surface reflectance and are of primary importance for the cell's open-circuit voltage because they allow reduction of the necessary thickness of the cell, and thereby the volume for bulk recombination (see eq. 3.1a).

Module design also influences optical design. Low-concentration approaches (*e.g.* prismatic covers) and bifacial cells are additional means to improve optical absorptance, but these will be omitted from the subsequent discussion.

3.3.1 Light trapping

Light trapping has been extensively studied in the context of Si solar cells. The indirect band gap of Si results in an absorption coefficient that is lower than 10^4 cm^{-1}

Physics of Semiconductor Devices

SECOND EDITION

S. M. Sze

Bell Laboratories, Incorporated
Murray Hill, New Jersey

A WILEY-INTERSCIENCE PUBLICATION

JOHN WILEY & SONS

New York • Chichester • Brisbane • Toronto • Singapore

Library of Congress Cataloging in Publication Data:

Sze, S. M., 1936-
Physics of semiconductor devices.
"A Wiley-Interscience publication."
Includes index.
1. Semiconductors. I. Title.

TK7871.85.S988 1981 537.6'22 81-213
ISBN 0-471-05661-8 AACR2

Printed in the United States of America

30 29 28 27 26

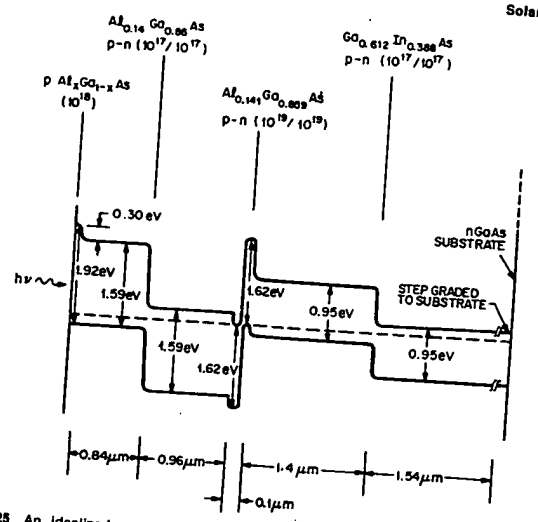

Fig. 25 An idealized cascade two-junction solar cell. (After Lamorte and Abbott, Ref. 31.)

have been obtained. For n-ITO/p-InP solar cells, efficiency of 14% under AM2 conditions has been obtained.[30]

A high-efficiency cascade heterojunction solar cell has been proposed.[31] An idealized band diagram is shown in Fig. 25. The device consists of a wide-gap cell (1.59 eV) and a narrow-gap cell (0.95 eV) joined by a heterojunction tunnel diode formed as an integral part of a monolithic structure. The design also includes a heteroface window layer to minimize surface recombination losses. Light that passes through the first cell without being absorbed will go through the ultrathin tunnel diode and be collected by the narrow-gap cell. By proper choice of bandgaps, the two cells can be designed for equal operating current. The theoretical efficiency under AM1.5 conditions at room temperature is over 30%.

14.4.2 Schottky-Barrier and MIS Solar Cells

The basic characteristics of Schottky-barrier diodes have been described in Chapter 5. A schematic energy diagram of a Schottky-barrier solar cell

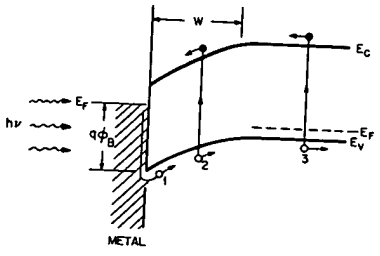

Fig. 26 Energy-band diagram of a Schottky-barrier solar cell under illumination.

under illumination is shown in Fig. 26. The metal must be thin enough to allow a substantial amount of the light to reach the semiconductor. There are three photocurrent components. Light with energy $h\nu > q\phi_B$ (the barrier height) can be absorbed in the metal and excite holes over the barrier into the semiconductor (1 in Fig. 26). This process is used in the photoelectric measurement of barrier height as described in Chapter 5. Short-wavelength light entering the semiconductor is mainly absorbed in the depletion region (2 in Fig. 26). Long-wavelength light is absorbed in the neutral region, creating electron–hole pairs just as in a p-n junction; the electrons must diffuse to the depletion edge to be collected (3 in Fig. 26). For solar-cell applications, the excitation of carriers from the metal into the semiconductor contributes less than 1% to the total photocurrent and, therefore, can be neglected.

The advantages of Schottky barriers include (1) low-temperature processing because no high-temperature diffusion is required; (2) adaptability to polycrystalline and thin-film solar cells; (3) high radiation resistance due to high electrical field near the surface; and (4) high-current output and good spectral response, because the presence of a depletion region right at the semiconductor surface can substantially reduce the effects of low lifetime and high recombination velocity near the surface.

The two major contributions to the spectral response and to the photocurrent come from the depletion region and the base neutral region. The collection from the depletion region is similar to that of a p-n junction. The high field in the depletion region will sweep the photogenerated carriers out before they can recombine, leading to a photocurrent:

$$J_\phi = qT(\lambda)F(\lambda)[1-\exp(-\alpha W)] \tag{41}$$

where $T(\lambda)$ is the transmission coefficient of the metal for the monochromatic light of wavelength λ. The photocurrent from the base region is

given by an expression identical to Eq. 26, except that $(1-R)$ is replaced by $T(\lambda)$, and $\alpha(x_j+W)$ by αW. If the back contact is ohmic and the device thickness is much greater than the diffusion length $H' \gg L_p$, the photocurrent from the base region is simplified to

$$J_n = qT(\lambda)F(\lambda)[\alpha L_n/(\alpha L_n+1)]\exp(-\alpha W). \tag{42}$$

The total photocurrent is given by the sum of Eqs. 41 and 42. To increase the photocurrent, one should increase the transmission coefficient T and diffusion length L_n. The spectral response for an ideal Schottky barrier is similar to those shown in Fig. 11*b* for $S_n < 10^4$ cm/s. The magnitude at each photon energy is lowered by reflection and absorption of light in the metal film. The transmission coefficient for gold films (10 to 100 Å) with an antireflection coating can reach 90 to 95%.

The I–V characteristics of a Schottky barrier under illumination is given by

$$I = I_s(e^{qV/nkT}-1) - I_L \tag{43}$$

and

$$I_s = AA^{**}T^2\exp(-q\phi_B/kT) \tag{44}$$

where n is the ideality factor, A the area, A^{**} the effective Richardson constant (refer to Chapter 5), and $q\phi_B$ the barrier height. The conversion efficiency is given by Eq. 11. For a given semiconductor, the efficiency can be calculated from Eqs. 11, 42, and 43 as a function of the barrier height. Figure 27 shows the ideal efficiency assuming zero reflection, unity ideality factor ($n=1$), and no resistance losses.[32] The efficiency increases with barrier height and, taking $q\phi_B(\max) = E_g$ as the limiting case, the maximum efficiency is about 25%. This figure is comparable to that of a homojunction.

To achieve high barrier heights on semiconductors, one usually uses metals with high work functions for n-type and low work functions for p-type, for example, 50 Å copper/50 Å chromium (Cr) on p-type Si, where chromium forms the Schottky barrier and copper serves as a protective coating.[33] For most metal–semiconductor systems made on uniformly doped substrates, the maximum barrier height is about $\frac{1}{3}E_g$. However, the barrier height can be increased to near the bandgap energy by inserting a heavily doped, thin semiconductor layer (100 Å with opposite doping to the substrate) between the metal and semiconductor substrate. The energy diagram for a metal–p^+-n Schottky barrier is shown[34] in the insert in Fig. 28. The effective barrier height is given by

$$q\phi_B = q\phi_m - q\chi + qV_{pm} \tag{45}$$

where $q\phi_m$ is the metal work function, χ the semiconductor electron affinity, and V_{pm} is the potential maximum given by

$$V_{pm} = \left(\frac{q}{2\epsilon_s N_A}\right)(N_A W_p - N_D W_n)^2. \tag{46}$$

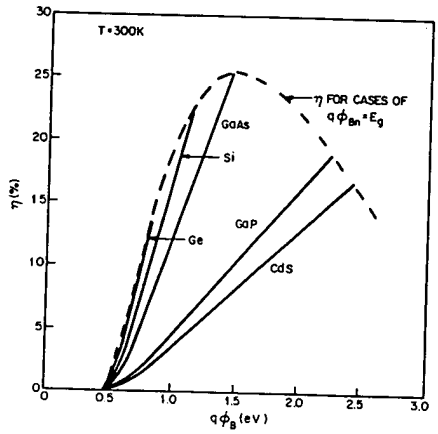

Fig. 27 Conversion efficiency versus barrier height. The envelope shows maximum efficiency calculated for $q\phi_B = E_g$. (After Pulfrey and McOuat, Ref. 32.)

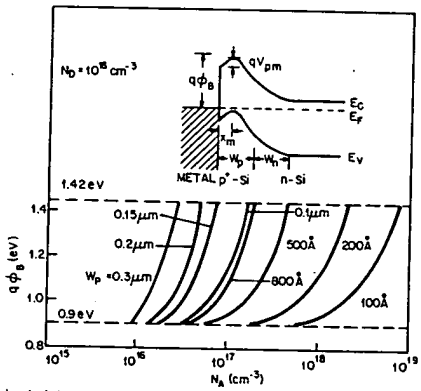

Fig. 28 Barrier height versus doping concentration and thickness of the p layer for a Au–GaAs Schottky-barrier solar cell. The insert shows the energy-band diagram of the metal–p^+-n device. (After Li, Ref. 34.)

The system described above is derived assuming $N_A W_p \gg N_D W_n$, so that the thin p region remains fully ionized and the potential maximum exists inside the p region. A complementary metal–n^+-p device can be made by interchanging n with p. The calculated GaAs barrier height for $N_D = 10^{16}\,\text{cm}^{-3}$ is shown in Fig. 28 as a function of N_A and W_p. Note that when $N_A W_p \geq 2 \times 10^{12}\,\text{cm}^{-2}$, the barrier height approaches the GaAs bandgap. The heavily doped surface layer can be formed by ion implantation and molecular-beam epitaxy. Another method is by a simple metallurgical reaction. The Schottky-barrier height of Al–n-type Si contact increases from 0.68 eV to about 0.9 eV under heat treatment ($< 580°C$). A thin recrystalized p^+ layer (~ 100 Å) containing $\geq 10^{19}\,\text{cm}^{-3}$ aluminum acceptors is formed;[35] and the band diagram is that shown in Fig. 28.

In an MIS solar cell, a thin insulating layer is formed between the metal and semiconductor substrate. The advantages of MIS solar cells include an electric field extending to the semiconductor surface in a direction that aids in collecting minority carriers generated by short-wavelength light, and the fact that the active region of the cells is free of the diffusion-induced crystal damage inherent in diffused p-n junction cells. The saturation current density is similar to that for Schottky barrier with an additional tunneling term (refer to Chapter 9):

$$J_s = A^{**}T^2 \exp(-q\phi_B/kT) \exp[-(q\phi_T)^{1/2}\delta] \tag{47}$$

where $q\phi_T$ in eV is the average barrier height presented by the insulating layer and δ in Å is the insulator thickness. Substitution of $V = V_{oc}$ and $J = 0$ in Eq. 43 yield,

$$V_{oc} = \frac{nkT}{q}\left[\ln\left(\frac{J_L}{A^{**}T^2}\right) + \frac{q\phi_B}{kT} + (q\phi_T)^{1/2}\delta\right]. \tag{48}$$

Equation 48 shows that V_{oc} of an MIS solar cell will increase with increasing δ. However, as the insulator thickness δ increases, the short-circuit current will decrease, causing a degradation of the conversion efficiency. An optimum oxide thickness for a metal–SiO_2–Si system is found[36] to be about 20 Å.

The aforementioned MIS solar cell has a uniform ultrathin metal layer covering the entire surface. A novel approach uses a thick metal MIS grid pattern with the semiconductor between the grid fingers covered by a transparent dielectric layer, shown[37] in Fig. 29. The 1000-Å SiO_2 serves as the transparent dielectric layer and as an antireflection coating. This structure is different from the ITO-Si heterojunction, since SiO_2 is non-conducting, and all currents flow through the tunneling MIS grid fingers. If positive fixed charges are in the oxide, an inversion layer will be formed at the semiconductor surface in addition to the surface depletion layer. The tunneling MIS grid with 20- to 30-Å SiO_2 will collect the photogenerated minority carriers (electrons for p-type substrate) from both the inversion and depletion layers. The inversion layer can also screen the surface

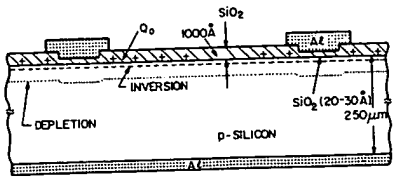

Fig. 29 Cross section of a solar cell having an MIS grid pattern. (After Van Halen et al., Ref. 37.)

recombination centers. At AM1, efficiencies of up to 18% have been obtained.[49,50] Since the oxide can be formed at low temperatures and no diffusion process is involved, this structure fabricated on polycrystalline or amorphous substrates is expected to provide a cost-effective solution for terrestrial applications.

14.4.3 Thin-Film Solar Cells

In thin-film solar cells, the active semiconductor layers are polycrystalline or disordered films that have been deposited or formed on electrically active or passive substrates, such as glass, plastic, ceramic, metal, graphite, or metallurgical silicon. A thin film of CdS, Si, GaAs, InP, CdTe, and so on, can be deposited onto the substrate by various methods, such as vapor growth, evaporation plasma, and plating. If the semiconductor thickness is larger than the inverse of the absorption coefficient, most light will be absorbed; if the diffusion length is larger than the film thickness, most photogenerated carriers can be collected.

The main advantage of thin-film solar cells is their promise of low cost, due to low-cost processing, and the use of relatively low cost materials. The main disadvantages are low efficiency and long-term instability. The low efficiency is partly caused by the grain boundary effect and partly caused by the poor quality of the semiconductor material grown on foreign substrates. The stability problem is caused by the chemical reaction of the semiconductor with ambient (such as O_2 and water vapor). Steps must be taken to ensure device reliability.

A schematic thin-film CdS solar cell is shown[38] in Fig. 30. The cells are fabricated using a substrate of electro-formed copper, coated with 0.5 μm of zinc. A layer of CdS about 20 μm thick is evaporated onto the heated substrate at 220°C. Reacting the CdS film in a cuprous ion solution forms a Cu_2S layer of 1000 Å. A transparent grid contact is deposited onto the Cu_2S and an antireflection layer applied over the Cu_2S. Figure 31 shows the energy diagram of the Cu_2S–CdS cell.[39] It is basically a heterojunction with